^{1}H Chemical Shift Imaging Reveals Loss of Brain Tumor Choline Signal after Administration of Gd-Contrast

Paul E. Sijens, Martin J. van den Bent, Peter J. C. M. Nowak, Pieter van Dijk, Matthijs Oudkerk

^{1}H MR spectra obtained by chemical shift imaging (CSI) of contrast-enhancing brain tumors before and after the administration of Gd-contrast agent were quantitated and compared with the results in normal brain tissue included in the volume of interest. Twenty-seven combined magnetic resonance imaging and spectroscopy (MRI, MRS) examinations of brain tumor lesions included T_1-weighted MRI and CSI (*TR/TE* 1500/135 ms double-spin echo) repeated 5–10 min after the administration of Gd-contrast agent (0.1–0.2 m*M*). In ^{1}H MR spectra of contrast-enhancing tumor Gd-contrast induced a mean loss of 15% of the peak area of choline-containing compounds (Cho, $P < 0.001$) that was correlated with precontrast Cho linewidth ($r = -0.72$, $P < 0.00001$). This phenomenon limits the diagnostic use of brain tumor MRS examinations performed immediately after contrast-enhanced MRI.

Key words: brain tumors; Gd-contrast agent; magnetic resonance imaging; magnetic resonance spectroscopy.

INTRODUCTION

With the availability of automated procedures for ^{1}H MR spectroscopy, brain MRS examinations have become easy, reliable, and fast. While demand for combined MRI/MRS examinations has increased, at this time MRS acquisition is not yet given priority over obtaining contrast-enhanced MRI. For the diagnostic use of MRS, it is therefore important to know whether the spectra obtained shortly after the administration of MRI contrast are similar to those before contrast.

Two recent single-voxel MRS studies (1, 2) have contradicted the suggestion that Gd-contrast causes artifacts (in spectra) associated with field inhomogeneity (3). Gd-contrast uptake did not affect Cho, creatine (Cr), and *N*-acetyl aspartate (NAA) peak areas in echo time (*TE*) 20 and 288 ms ^{1}H MR spectra of tumors and Gd-enhancing multiple sclerosis plaques (1, 2). It has been shown, however, that in single-voxel MRS studies, it can be difficult to demonstrate the significance of spectral changes due to variations in the sensitivity of the MR system (4). The purpose of this study is to quantitate and compare arrays of ^{1}H CSI spectra obtained in brain cancer patients before and after the administration of Gd-contrast agent. The use of CSI rather than single voxel techniques is expected to facilitate the detection of small contrast-induced spectral changes by allowing direct comparison of possible effects on Gd-enhancing tumor regions and other brain tissue included in the volume of interest (VOI).

MATERIALS AND METHODS

Reported are the results of 27 combined MRI/MRS examinations of Gd-enhancing brain tumor lesions. Data are from 17 patients (13 primary brain tumors, 4 metastatic brain tumors) with inclusion of MRI/MRS examinations repeated at different months ($n = 9$) and a second tumor in one case ($n = 1$) adding up to the total of 27. MRI/MRS was performed at 1.5 T by using the standard head coil of a Siemens Magnetom Vision MR scanner (Siemens AG, Erlangen, Germany). MRI included a T_1-weighted spin-echo sequence (*TR/TE* 570/14 ms) repeated after the administration of Gd-contrast agent (randomized between 0.1–0.2 m*M* Magnevist (Gd-DTPA, Schering AG, Berlin, Germany) or Dotarem (Gd-DOTA, Guerbet SA, Paris, France). An automated hybrid 2D CSI sequence (*TR/TE* 1500/135 ms PRESS double-spin echo) was used for MRS, before and (under identical measurement conditions) 5–10 min after the contrast. Hybrid CSI includes preselection of a volume that is located within the brain to prevent the strong interference from subcutaneous fat and is smaller than the phase-encode field of view that must be large enough to prevent wraparound artifacts. Administration of the Gd-contrast medium through an infusion system allowed the patient to remain within the magnet and thus keep exactly the same position relative to head coil and magnetic field. The CSI sequence produced a 16 × 16 transversely oriented matrix that was defined by phase encoding with a field of view of 16 × 16 cm. The plane was positioned to include the abnormality within the VOI resulting in maps of up to 8 × 10 spectra (VOI 8 × 10 × 2 cm), selected with respective field gradients of 0.8, 0.8, and 3.0 mT/m. The field homogeneity achieved in automated non-localized multiple angle projection (MAP) shimming resulted in water peak linewidths of typically less than 8 Hz in the VOI. Spectral maps were collected with 2.56 ms sinc-hanning-shaped RF pulses preceded by 25.6 ms Gaussian-shaped RF pulses for chemical shift selective excitation (CHESS) and subsequent spoiling of the resultant water signal. The second spin echo was collected by using 1024 data points and a spectral width of 500 Hz. All hybrid PRESS 2D CSI measurements were one acquisition per phase encode step with four prescans and $TR = 1500$ ms (acquisition time 6:31 min). After retrospective positioning

MRM 37:222–225 (1997)

From the Dr. Daniel den Hoed Cancer Center, Departments of Radiology (P.E.S., P.v.D., M.O.), Neurology (M.J.v.d.B.), and Radiation Therapy (P.J.C.M.N.), University Hospital Rotterdam, Rotterdam, The Netherlands.

Address correspondence to: Paul E. Sijens, Ph.D., Department of Radiology, Dr. Daniel den Hoed Cancer Center, University Hospital Rotterdam, Groene Hilledijk 301, 3075 AE Rotterdam, The Netherlands.

Received April 18, 1996; revised June 10, 1996; accepted July 26, 1996.

0740-3194/97 $3.00

of voxels on tumor, time domain data were multiplied with a Gaussian function (center 0 ms, half width 256 ms), 2D Fourier transformed, phase and baseline corrected and quantitated by means of frequency domain curve fitting with the assumption of Gaussian lineshapes, using the standard Numaris-3 software package provided with the MR system. In the curve fitting the number of peaks and their chemical shift ranges were fixed whereas linewidths and peak intensities were unrestricted. The results of automated phase and baseline correction were generally good; manual fine adjustment of the phase and of the peak ranges excluded in the (spline) baseline correction was needed in a minority of cases. Postcontrast Cho, Cr, and NAA peak areas of one or more tumor voxels, i.e., all voxels containing Gd-enhancing tumor, were averaged and divided by the mean areas of the same voxels before contrast. Also quantitated and averaged were the results obtained in, depending on the amount of normal brain tissue in the VOI, 3 to 10 unaffected brain voxels before and after contrast.

RESULTS

Representative spectra of a (8, 9-labeled) CSI voxel containing primary brain tumor before and after administration of Gd-contrast agent are shown in Fig. 1. After contrast there is a 20% reduction of Cho in Gd-enhancing tumor. For all patients combined the peak areas of brain metabolites in Gd-enhancing tumor and in contralateral normal brain tissue after the administration of contrast relative to the respective values before contrast are presented in Table 1. The large standard deviations in the

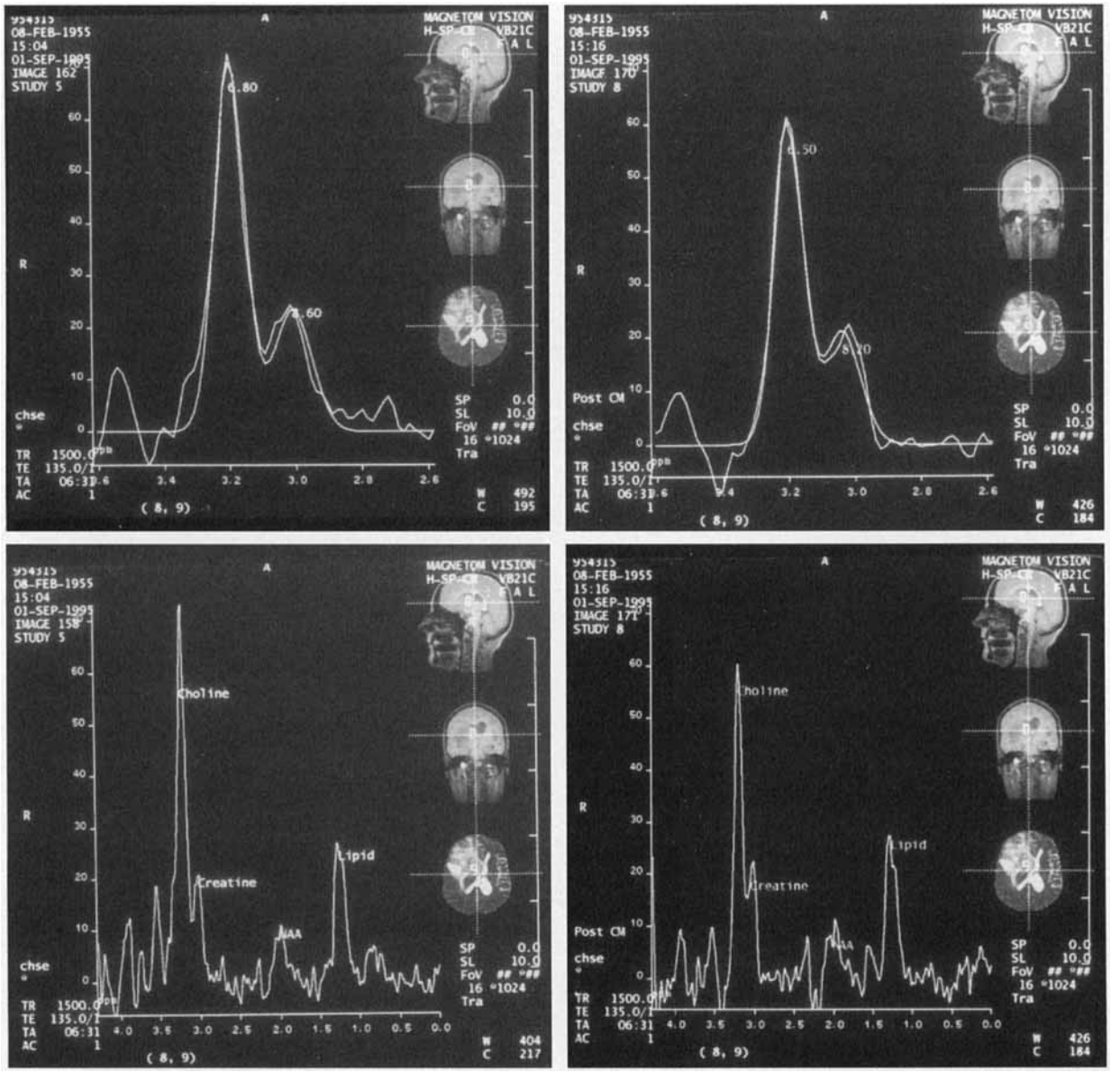

FIG. 1. CSI localized MR spectrum of 2 cm^3 voxel containing recurrent astrocytoma with subregion showing the fitted Cho linewidths before ((a) 6.8 Hz) and after ((b) 6.5 Hz) administration of Gd-contrast agent. Acquisition time: 6:31 min (*TE/TR* 135/1500).

Table 1
Metabolite Peak Areas after Contrast Relative to Respective Values before Contrast (Precontrast = 100%; Means ± SD, n = 27)

	Cho	Cr	NAA
Gd-enhancing tumor	85 ± 18[a]	101 ± 42	117 ± 42
Unaffected brain (from same VOI as tumor)	96 ± 16	101 ± 21	102 ± 12
Quotient of area in Gd-enhanced tumor and total signal (Cho + Cr + NAA) in unaffected brain	85 ± 24[b]	103 ± 49	116 ± 43

[a] $P < 0.001$ (t test, paired samples).
[b] $P < 0.01$ (t test, paired samples).

tumor Cr and NAA areas reflect the generally low levels of these metabolites in tumor. The change in tumor Cho peak area is significant both when considered separately ($P < 0.001$) and when divided by the change of total signal (Cho + Cr + NAA) in the unaffected brain included in the VOI ($P < 0.01$, Table 1). Gd-contrast administration did not induce any significant change in the linewidth and chemical shift of Cho, Cr, or NAA in tumor or control brain tissue. Nevertheless, there was a trend that tumor Cho signals that are broadened compared with control tissue decrease after administration of Gd-contrast (Fig. 1, upper part).

Regression analyses revealed significant correlation between postcontrast tumor Cho peak area and precontrast Cho linewidth ($r = -0.73$, $P < 0.00001$). This correlation is shown in Fig. 2. The Cho linewidth in control brain tissue showed little variation between cases (4.4 ± 0.6 Hz). Peak areas of the lactate doublet at 1.32 ppm (inverted at TE = 135 ms) or lipid signals (1.30 ppm), detected in a number of cases, were not significantly affected by the administration of contrast medium.

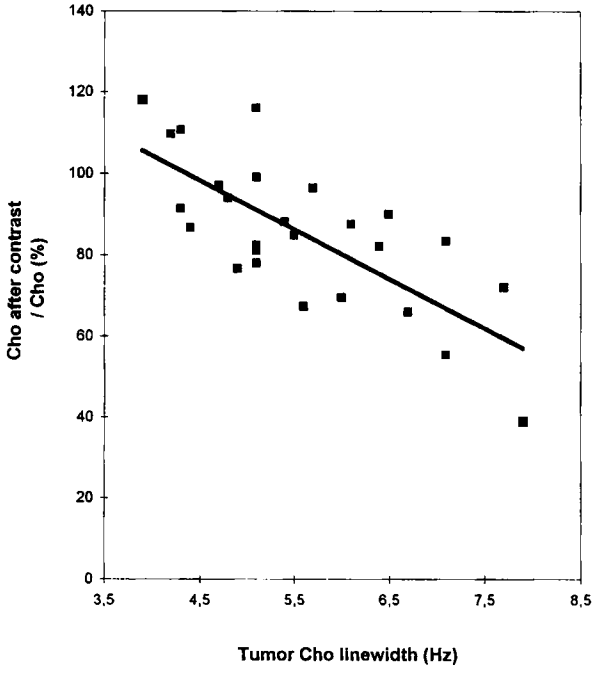

FIG. 2. Cho peak area after Gd-contrast administration as a function of tumor Cho linewidth ($r = -0.73$, $P < 0.00001$).

DISCUSSION

^{1}H MR spectra of brain tumors are characterized by increased Cho and absence of NAA (5–14). Relative to that in unaffected contralateral brain tissue Cho peak area is generally increased in brain tumor, but rarely more than by a factor of two (15, 16). For the diagnostic use of MRS in tumor analysis performed immediately after Gd-enhanced MRI, it is therefore important to realize the impact of Gd-contrast on the peak areas of Cho and other metabolites in tumor, even if the effects are moderate. As can be deduced from the 85 ± 18 percentage of post-Gd tumor Cho relative to pre-Gd Cho (Table 1), the loss of tumor Cho signal varied considerably between individuals from around zero to 40%. These figures imply that Gd administration may turn a tumor Cho peak area of 200% of that in control brain tissue into a less distinct 170% or even into a diagnostically meaningless peak area of 120%. The mean 15% loss of tumor Cho peak area after Gd-contrast disagrees with the recent single-voxel MRS study reporting that Gd-contrast administration does not significantly affect tumor Cho, Cr, and NAA peak areas in both TE 20 and TE 288 ms single-voxel MR spectra (1). In view of this it must be noted that a moderate change in tumor Cho signal is difficult to demonstrate with single voxel techniques if there are variations in the sensitivity of the MR system (4) and, if both tumor and control voxels are measured, due to decreasing reproducibility of voxel localization because of extended examination times.

The finding that the signal-to-noise ratio and resolution of the spectra remained similar after Gd-contrast administration is in agreement with recent studies (1, 2) and contradicts the suggestion that Gd-contrast causes artifacts (in spectra) associated with field inhomogeneity (3). The highly significant correlation between precontrast Cho linewidth and postcontrast Cho peak area in percent of precontrast Cho (Fig. 2) implies that tumor Cho signals that are broadened compared with control tissue, decrease after administration of Gd-contrast (Fig. 1, upper part). Our hypothesis is that Gd-contrast causes T_2-shortening of an extracellular choline containing tumor component resulting in a loss of MRS detectable Cho. In that case, mean contrast induced loss of tumor Cho signal would be expected to be larger than 15% in MRS protocols employing TE's longer than 135 ms and smaller than 15% (or negligible) in STEAM or PRESS studies employing (very) short TE's. The selective loss of Cho would fit in with the knowledge that the NAA and

Cr signals in tumor spectra are primarily contributed by non-tumor tissue with intact blood-brain barrier (partial volume effect).

It is concluded that in combined MRI/MRS examinations of brain tumors MRS measurements are preferably not performed shortly after contrast-enhanced MRI. While the signal-to-noise ratio and resolution of spectra remains similar, there is a potential decrease in tumor characteristic Cho signal that may interfere with the diagnostic use of the examination. If in combined MRI/MRS examinations for tumor analysis MRS is only performed after Gd-contrast and the presence of vital tumor remains ambiguous, for instance a doubtful Cho increase in Gd-enhancing abnormality, it is advised to repeat MRS in a separate examination without Gd-administration.

ACKNOWLEDGMENTS

The authors thank Peter Kappert for participating in the data acquisition.

REFERENCES

1. J. S. Taylor, W. E. Reddick, P. B. Kingsley, R. J. Ogg, Proton MRS after gadolinium contrast agent, *in* "Proc., SMR, 3rd Annual Meeting, Nice, 1995," p. 1854.
2. P. A. Narayana, J. S. Wolinsky, E. F. Jackson, M. McCarthy, Proton MR spectroscopy of gadolinium-enhanced multiple sclerosis plaques. *J. Magn. Reson. Imaging* **2,** 263–270 (1992).
3. J. R. Alger, J. A. Frank, A. Bizzi, M. J. Fulham, B. X. DeSouza, M. O. Duhaney, S. W. Inscoe, J. L. Black, P. C. M. van Zijl, C. T. W. Moonen, G. Di Chiro, Metabolism of human gliomas: assessment with H-1 MR spectroscopy and F-18 fluorodeoxyglucose PET. *Radiology* **177,** 633–641 (1990).
4. E. T. Kariakopoulos, C. A. Stewart, B. M. Guthrie, R. Walcarius, D. J. Mikulis, The effect of Gd-DTPA on proton spectroscopy in the normal human brain, *in* "Proc., SMR, 2nd Annual Meeting, San Francisco, 1994," p. 566.
5. D. L. Arnold, E. A. Shoubridge, J.-G. Villemure, W. Feindel, Proton and phosphorus magnetic resonance spectroscopy of human astrocytomas in vivo; preliminary observations of tumor grading. *NMR Biomed.* **3,** 184–189 (1990).
6. H. Bruhn, J. Frahm, M. L. Gyngell, K. D. Merbold, W. Hänicke, R. Sauter, C. Hamburger, Noninvasive differentiation of tumors with use of localized H-1 MR spectroscopy in vivo: initial experience in patients with cerebral tumors. *Radiology* **172,** 541–548 (1989).
7. P. Demaerel, K. Johannik, P. Van Hecke, C. Van Ongeval, S. Verellen, G. Marchal, G. Wilms, C. Plets, J. Goffin, F. Van Calenberg, M. Lammens, A.L. Beart, Localized ^{1}H NMR spectroscopy in fifty cases of newly diagnosed intracranial tumors. *J. Comput. Assist. Tomogr.* **15,** 67–76 (1991).
8. S. S. Gill, D. G. T. Thomas, N. Van N. Bruggen, D. G. Gadian, C. J. Peden, J. D. Bell, I. J. Cox, D. K. Menon, R. A. Iles, D. J. Bryant, G. A. Coutts, Proton MR spectroscopy of intracranial tumours: in vivo and in vitro studies. *J. Comput. Assist. Tomogr.* **14,** 497–504 (1990).
9. H. Kugel, W. Heindel, R.-I. Ernestus, J. Bunke, R. du Mesnil, G. Friedmann, Human brain tumors: spectral patterns detected with localized H-1 MR spectroscopy. *Radiology* **183,** 701–709 (1992).
10. P. R. Luyten, A. J. H. Marien, W. Heindel, P. H. J. van Gerwen, K. Herholz, J. A. den Hollander, Metabolic imaging of patients with intracranial tumors: H-1 MR spectroscopic imaging and PET. *Radiology* **176,** 791–799 (1990).
11. M. J. Fulham, A. Bizzi, M. J. Dietz, H. H.-L. Shih, R. Raman, G. S. Sobering, J. A. Frank, A. J. Dwyer, J. R. Alger, G. Di Chiro, Mapping of brain tumor metabolites with proton MR spectroscopic imaging: clinical relevance. *Radiology* **185,** 675–686 (1992).
12. D. Ott, J. Hennig, T. Ernst, Human brain tumors: assessment with in vivo proton MR spectroscopy. *Radiology* **186,** 745–752 (1993).
13. C. M. Segebarth, D. F. Baleriaux, P. R. Luyten, J. A. den Hollander, Detection of metabolic heterogeneity of human intracranial tumors in vivo by ^{1}H spectroscopic imaging. *Magn. Reson. Med.* **13,** 62–76 (1990).
14. P. E. Sijens, M. V. Knopp, A. Brunetti, K. Wicklow, B. Alfano, P Bachert, J. A. Sanders, A. E. Stillman, H. Kett, R. Sauter, M. Oudkerk, ^{1}H MR spectroscopy in patients with metastatic brain tumors: a multi-center study. *Magn. Reson. Med.* **33,** 818–826 (1995).
15. J.-P. R. Usenius, R. A. Kauppinen, P. A. Vainio, J. A. Hernesniemi, M. P. Vapalahti, L. A. Paljärvi, S. Soimakallio, Quantitative metabolite patterns of human brain tumors: detection by ^{1}H NMR spectroscopy in vivo and in vitro. *J. Comp. Assist. Tomogr.* **18,** 705–713 (1994).
16. P. E. Sijens, van P. Dijk, Oudkerk M, Correlation between choline level and Gd-DTPA enhancement in patients with brain metastases of mammary carcinoma. *Magn. Reson. Med.* **32,** 549–555 (1994).